

See discussions, stats, and author profiles for this publication at: <https://www.researchgate.net/publication/260215527>

# ChemInform Abstract: Chemical Vapor Deposition of Graphene Single Crystals

ARTICLE *in* ACCOUNTS OF CHEMICAL RESEARCH · FEBRUARY 2014

Impact Factor: 22.32 · DOI: 10.1021/ar4003043 · Source: PubMed

---

CITATIONS

39

---

READS

127

3 AUTHORS, INCLUDING:



**Zheng Yan**

University of Illinois, Urbana-Champaign

35 PUBLICATIONS 2,122 CITATIONS

SEE PROFILE



**Zhiwei Peng**

University of Maryland, College Park

49 PUBLICATIONS 1,466 CITATIONS

SEE PROFILE

# Chemical Vapor Deposition of Graphene Single Crystals

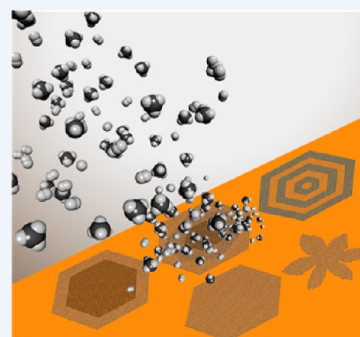
Zheng Yan,<sup>†</sup> Zhiwei Peng,<sup>†</sup> and James M. Tour<sup>\*,†,‡,§</sup>

<sup>†</sup>Department of Chemistry, <sup>‡</sup>Richard E. Smalley Institute for Nanoscale Science and Technology, <sup>§</sup>Department of Materials Science and NanoEngineering, Rice University, 6100 Main Street, Houston, Texas 77005, United States

**ABSTRACT:** As a two-dimensional (2D)  $sp^2$ -bonded carbon allotrope, graphene has attracted enormous interest over the past decade due to its unique properties, such as ultrahigh electron mobility, uniform broadband optical absorption and high tensile strength. In the initial research, graphene was isolated from natural graphite, and limited to small sizes and low yields. Recently developed chemical vapor deposition (CVD) techniques have emerged as an important method for the scalable production of large-size and high-quality graphene for various applications. However, CVD-derived graphene is polycrystalline and demonstrates degraded properties induced by grain boundaries. Thus, the next critical step of graphene growth relies on the synthesis of large graphene single crystals.

In this Account, we first discuss graphene grain boundaries and their influence on graphene's properties. Mechanical and electrical behaviors of CVD-derived polycrystalline graphene are greatly reduced when compared to that of exfoliated graphene. We then review four representative pathways of pretreating Cu substrates to make millimeter-sized monolayer graphene grains: electrochemical polishing and high-pressure annealing of Cu substrate, adding of additional Cu enclosures, melting and resolidifying Cu substrates, and oxygen-rich Cu substrates. Due to these pretreatments, the nucleation site density on Cu substrates is greatly reduced, resulting in hexagonal-shaped graphene grains that show increased grain domain size and comparable electrical properties as to exfoliated graphene. Also, the properties of graphene can be engineered by its shape, thickness and spatial structure. Thus, we further discuss recently developed methods of making graphene grains with special spatial structures, including snowflakes, six-lobed flowers, pyramids and hexagonal graphene onion rings. The fundamental growth mechanism and practical applications of these well-shaped graphene structures should be interesting topics and deserves more attention in the near future. Following that, recent efforts in fabricating large single-crystal monolayer graphene on other metal substrates, including Ni, Pt, and Ru, are also described. The differences in growth conditions reveal different growth mechanisms on these metals. Another key challenge for graphene growth is to make graphene single crystals on insulating substrates, such as h-BN,  $SiO_2$ , and ceramic. The recently developed plasma-enhanced CVD method can be used to directly synthesize graphene single crystals on h-BN substrates and is described in this Account as well.

To summarize, recent research in synthesizing millimeter-sized monolayer graphene grains with different pretreatments, graphene grain shapes, metal catalysts, and substrates is reviewed. Although great advancements have been achieved in CVD synthesis of graphene single crystals, potential challenges still exist, such as the growth of wafer-sized graphene single crystals to further facilitate the fabrication of graphene-based devices, as well as a deeper understanding of graphene growth mechanisms and growth dynamics in order to make graphene grains with precisely controlled thicknesses and spatial structures.



## 1. INTRODUCTION

During the past decade, graphene, a single layer of  $sp^2$ -bonded carbon atoms arranged in a honeycomb lattice, has attracted a plethora of attention because of its remarkable physical, mechanical and optical properties.<sup>1–4</sup> However, the simple exfoliation of graphene from graphite reported in the initial research is limited to micrometer sizes and low yield.<sup>1</sup> Reduced graphene oxide sheets made by self-assembly could provide a low-cost alternative with high throughput, but the as-made graphene films exhibit poor electrical properties.<sup>5</sup> In contrast, large-size and high-quality graphene can be grown epitaxially on silicon carbide.<sup>6</sup> However, silicon carbide wafers are relatively expensive. Moreover, the growth is performed at a high temperature ( $\sim 1500^\circ\text{C}$ ) under ultrahigh vacuum, increasing the energy cost of the growth process.

The recently developed chemical vapor deposition (CVD) method, using catalytic substrates, has emerged as a convenient technique to obtain high-quality and large-size graphene that can then be transferred onto arbitrary substrates using a polymer-assisted transfer process.<sup>7–10</sup> The CVD method is scalable and has been used to produce 30 in. sized graphene films on Cu foils (Figure 1a) using roll-to-roll based techniques.<sup>10</sup> However, CVD graphene is polycrystalline, and the grain boundaries are composed of aperiodic heptagon-pentagon pairs<sup>11</sup> (the left image in Figure 1b) or overlapped bilayer regions<sup>12</sup> (the right image in Figure 1b). The presence of grain boundaries in CVD graphene sheets could alter their mechanical and electrical behaviors. For example, indentation measurements performed

**Received:** December 19, 2013

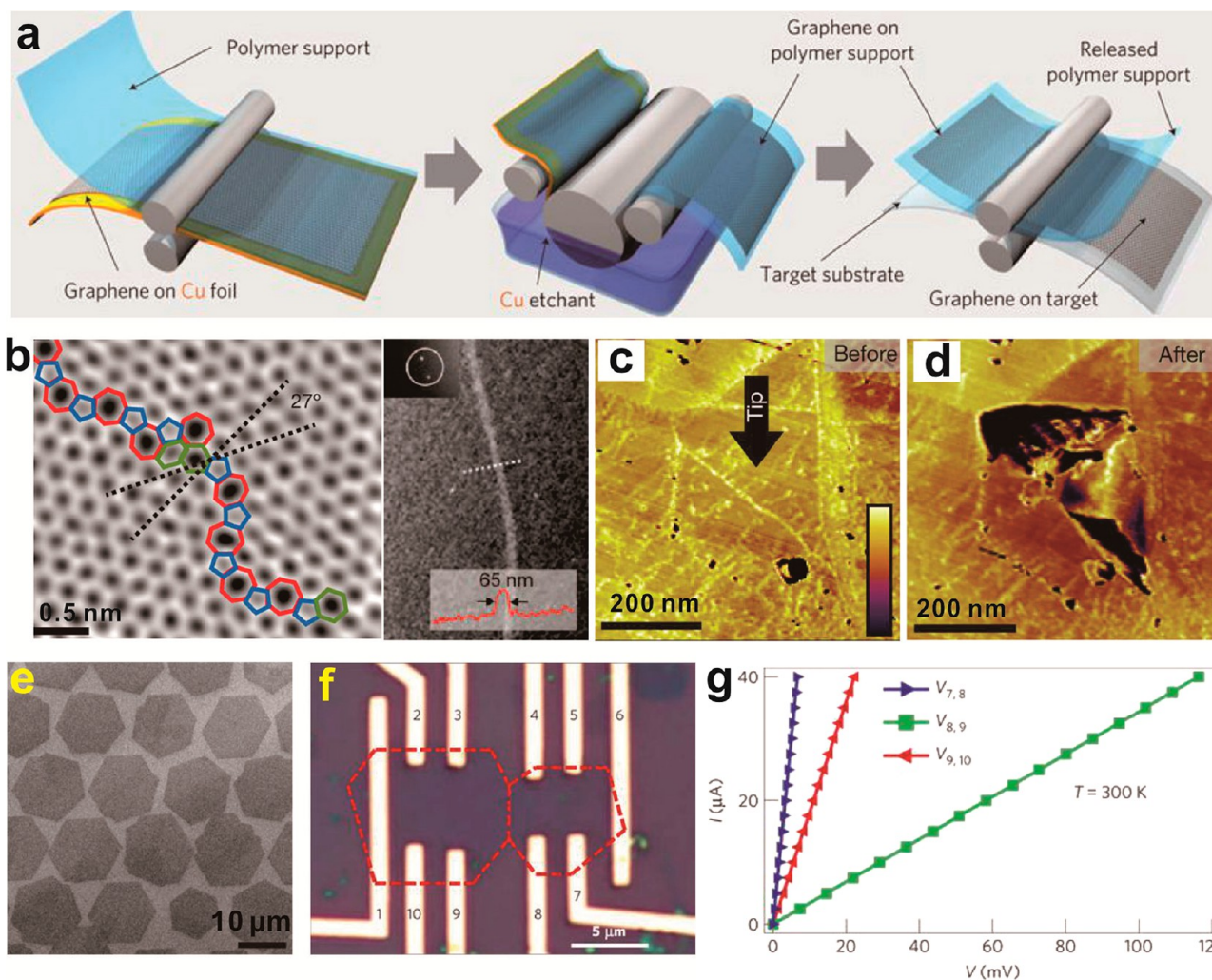


**Figure 1.** CVD graphene. (a) Schematic of the transfer of graphene produced on Cu using the roll-to-roll method. Adapted with permission from Macmillan Publishers Ltd. (*Nature*),<sup>10</sup> copyright 2010. (b) Two types of graphene boundaries: aperiodic heptagon-pentagon pairs (the left image, adapted with permission from Macmillan Publishers Ltd. (*Nature*),<sup>11</sup> copyright 2011) and overlapped bilayer regions (the right image, adapted with permission<sup>12</sup> from AAAS). (c, d) Tears occurred along the graphene grain boundaries after indentation. Adapted with permission from Macmillan Publishers Ltd. (*Nature*),<sup>11</sup> copyright 2011. (e) Hexagonal graphene grains made on Cu. (f) Hall bar device fabricated over two merged graphene domains. (g) Room-temperature  $I$ – $V$  curves measured within each graphene grain and across the grain boundary. Panels (e)–(g) are adapted with permission from Macmillan Publishers Ltd. (*Nat. Mater.*),<sup>14</sup> copyright 2011.

on polycrystalline CVD graphene films revealed that both their elastic modulus and breaking force were consistently reduced by an order of magnitude as compared to that of exfoliated graphene.<sup>13</sup> Atomic force microscope (AFM) characterizations in Figure 1c and d demonstrate that tears were often observed to occur along the graphene grain boundaries after indentation.<sup>11</sup> Thus, the synthesis of graphene without any grain boundaries, namely graphene single crystals or grain-free graphene, would be of higher value for future studies and practical applications of graphene in optics and electronics.

Recently, Yu et al. synthesized hexagonal monolayer graphene single crystals on Cu using Ar-diluted  $\text{CH}_4$  as the carbon source, with grain sizes of  $\sim 15\text{ }\mu\text{m}$  (Figure 1e).<sup>14</sup> The hexagonal crystallite shape of the graphene grains arises from the well-defined zigzag edges,<sup>15</sup> and has been shown to have interesting electronic properties. By inferring the locations of grain boundaries from two hexagonal grains which have merged (Figure 1f), electrical measurements show an increased resistance across the grain boundary (Figure 1g), which is attributed to the additional scattering caused by the grain

boundaries.<sup>14</sup> Tsen et al. found that the overall conductance and carrier mobility of polycrystalline CVD graphene could approach 90% that of single-crystal graphene if the graphene grains had well-stitched grain boundaries.<sup>12</sup>

Based on this discussion of graphene grain boundaries, it is apparent that increasing grain sizes is the key point to improve the quality of polycrystalline CVD graphene. In this Account, we will first describe four recently developed methods of making millimeter-sized hexagonal monolayer graphene grains on Cu substrates, which is the most popular substrate for graphene growth. Then, we will discuss the synthesis of graphene grains with special spatial structures, such as snowflake- and flower-like monolayer graphene grains, pyramid-like bi- and trilayer graphene grains, and hexagonal onion-ring-like graphene grains. In closing, we will review the efforts toward growing large single-crystal graphene on other substrates including Ni, Pt, Ru, and h-BN.



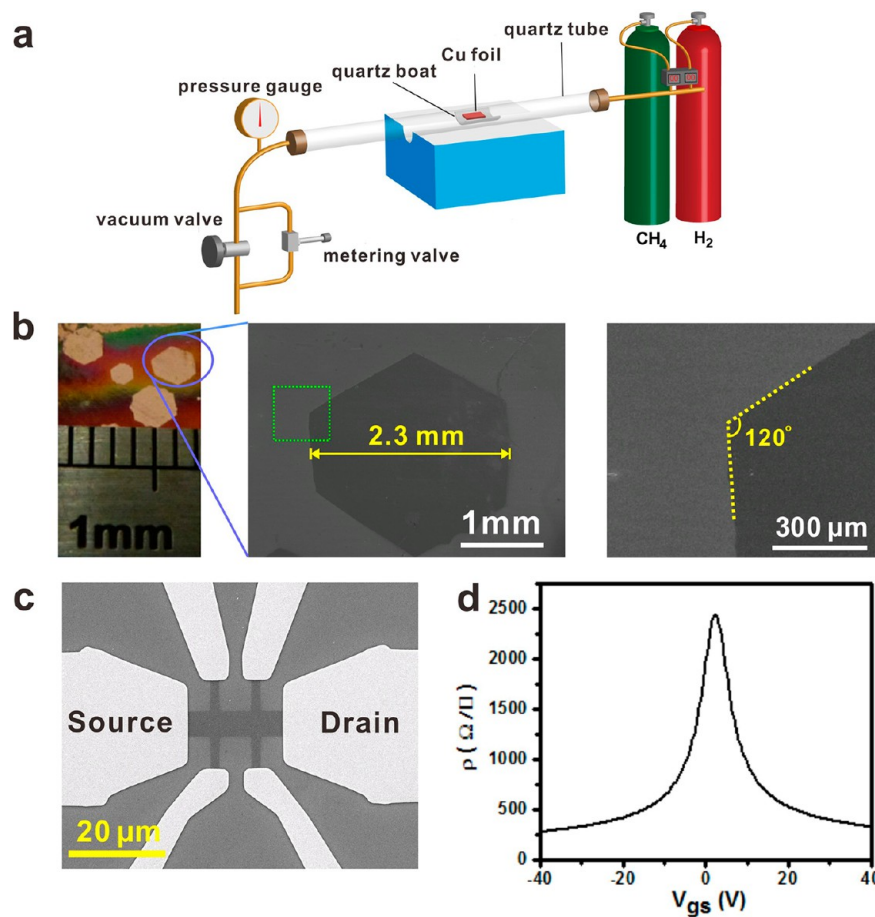


**Figure 2.** Millimeter-sized graphene grains made on polished and annealed Cu foils. (a) Schematic of the controlled pressure CVD system. (b) Typical optical and scanning electron microscope (SEM) images of as-produced millimeter-sized graphene grains on pretreated Cu foils. (c) Typical SEM image of a graphene Hall bar field-effect transistor (FET) on a SiO<sub>2</sub>/Si substrate. (d) Resistivity of graphene versus the back gate voltage. Reproduced with permission from ref 20. Copyright 2012 American Chemical Society.

## 2. GROWTH OF MILLIMETER-SIZED GRAPHENE SINGLE CRYSTALS ON Cu SUBSTRATES

The Cu-based CVD synthesis of graphene is a reliable method to obtain high-quality graphene films with controlled thickness.<sup>8,10,16</sup> Due to negligible carbon solubility, graphene growth is restricted to the Cu surface and is a seed-induced 2D growth.<sup>15</sup> The following elementary steps are expected for hydrocarbon (e.g., CH<sub>4</sub>) conversion to graphene on the surface of Cu during CVD growth: (i) adsorption of CH<sub>4</sub> on Cu surfaces; (ii) partial dehydrogenation of CH<sub>4</sub>, resulting in C species such as CH<sub>x</sub> ( $x = 0-3$ ); (iii) surface diffusion of C species on Cu surfaces; (iv) C species nucleation on the active sites of Cu to form graphene domains; (v) growth of graphene domains by adsorbing C species on their edges; (vi) coalescence of adjacent graphene domains to form polycrystalline graphene films.<sup>15,17-20</sup> Based on this growth mechanism, the key points to the growth of large single-crystal graphene is to slow graphene nucleation and reduce graphene grain densities so that only a small number of them, preferably only one crystal, would initiate. As of this writing, four different methods, the details of which follow, have been reported to pretreat Cu substrates for formation of millimeter-sized monolayer graphene grains. Because variation of other parameters such as growth temperature, chamber pressure, and H<sub>2</sub> to CH<sub>4</sub> ratios are generally explored in most graphene growth research, they will not be discussed in detail here.

### 2.1. Millimeter-Sized Monolayer Graphene Single Crystals Made on Electrochemical-Polished and High-Pressure Annealed Cu Foils

Commercial Cu foils are generally coated with protection layers, sharp wrinkles, step edges, and defects, which could work as active sites for graphene heteronucleation. Electrochemical polishing was used to remove the protection layers from Cu and then a pressure-controlled CVD system (Figure 2a) was used to anneal the electrochemical-polished Cu foils at 2 atm (H<sub>2</sub>) for 7 h to minimize sharp wrinkles and defects.<sup>20</sup> Using these pretreated Cu foils, ~2.3 mm sized hexagonal monolayer graphene grains with straight edges were synthesized (Figure 2b). The as-made single-crystal CVD graphene shows high-performance electronic properties, with a carrier (hole) mobility at ~11 000 cm<sup>2</sup> V<sup>-1</sup> s<sup>-1</sup>, comparable to that of exfoliated graphene (Figure 2c and d). Wu et al. reported the fabrication of ~1.2 mm sized hexagonal monolayer grains on mechanically and electrically polished, and atmospherically annealed Cu foils using solid carbon sources to trigger the growth.<sup>21</sup>

### 2.2. Millimeter-Sized Monolayer Graphene Single Crystals Made on the Inside of Enclosure-like Cu Structures

The Ruoff group developed enclosure-like Cu structures that can be used for the growth of large single-crystal graphene (Figure 3). They first demonstrated the successful synthesis of ~0.5 mm single-crystal monolayer graphene grains on the inside of Cu

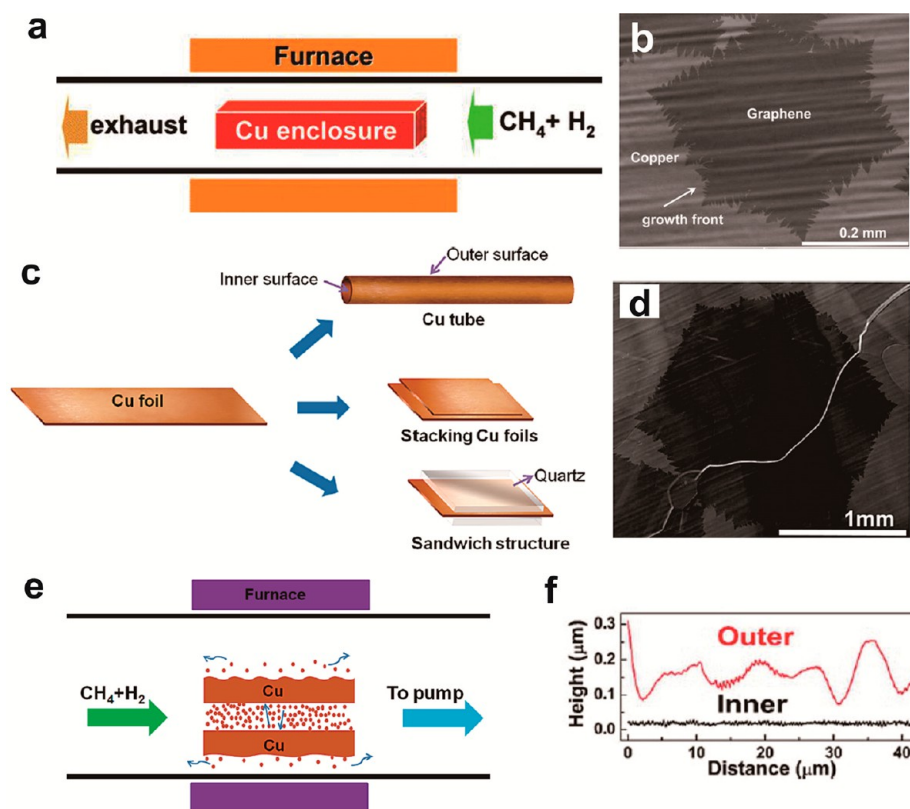


**Figure 3.** Millimeter-sized graphene grains made on the inside of enclosure-like Cu structures. (a) Schematic of Cu enclosures for graphene growth. (b) One SEM image of graphene grains grown on the inner surface of a Cu enclosure. Panels (a) and (b) were adapted with permission from ref 22. Copyright 2011 American Chemical Society. (c) Schemes of Cu tube, stacked Cu foils, and Cu foil between two quartz slides. (d) Typical SEM image of one graphene grain grown on the inner surface of the tube-like Cu structure. (e) Suppression of loss of Cu by evaporation due to redeposition of Cu in a confined space. (f) Height profiles on the inner surface (the black curve) and the outer surface (the red curve) of a tube-like Cu structure after annealing. Panels (c)–(f) are adapted with permission,<sup>23</sup> copyright © 2013 WILEY-VCH Verlag GmbH & Co. KGaA, Weinheim.

enclosures (Figure 3a and b).<sup>22</sup> The detailed mechanism was not explored.

In a second paper, Ruoff and co-workers reported the growth of  $\sim 2$  mm single-crystal monolayer graphene grains on the inside of Cu tubes (Figure 3c and d).<sup>23</sup> In this case, the Cu was electrochemically polished in advance before being rolled into tubes. Moreover, the authors explored the reasons for suppression of graphene nucleation on the inside of these tube-like Cu structures. They proposed that the redeposition of Cu in the confined space could help the Cu inner surfaces remain flat (Figure 3e). AFM measurements support this assumption and indicate that the inner Cu surfaces are much smoother than the outer surfaces with less defect sites (Figure 3f). Thus, graphene nucleation on inner surfaces could be suppressed, leading to the formation of millimeter-sized graphene single crystals.

### 2.3. Millimeter-Sized Monolayer Graphene Single Crystals Made on Resolidified Cu

Recently, Geng et al. and Wu et al. tried growing large graphene crystallites on liquid Cu by increasing growth temperatures above the melting point of Cu.<sup>24,25</sup> Although isolated hexagonal graphene grains could be made using this method, the grain sizes of the as-made graphene were limited to  $200\ \mu\text{m}$ , possibly due to the gradient in carbon concentration during cooling that leads to convection within the liquid Cu.<sup>26</sup>

Mohsin et al. modified this method and used a two-step process, melting and resolidifying Cu, to pretreat the Cu substrates (the left image in Figure 4a).<sup>26</sup> On this pretreated Cu,

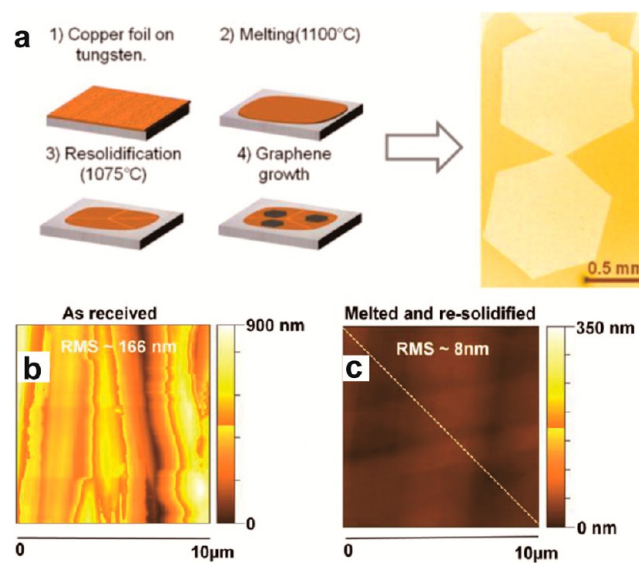


**Figure 4.** Millimeter-sized graphene grains made on resolidified Cu. (a) Schematic of resolidifying Cu on a tungsten substrate (left) and one optical image of millimeter-sized hexagonal graphene grains grown on resolidified Cu (right). AFM topographical images of various copper surfaces: (b) as-received and (c) resolidified. Reproduced with permission from ref 26. Copyright 2013 American Chemical Society.

$\sim 1$  mm sized hexagonal monolayer graphene grains were successfully prepared (the right image in Figure 4a). The authors

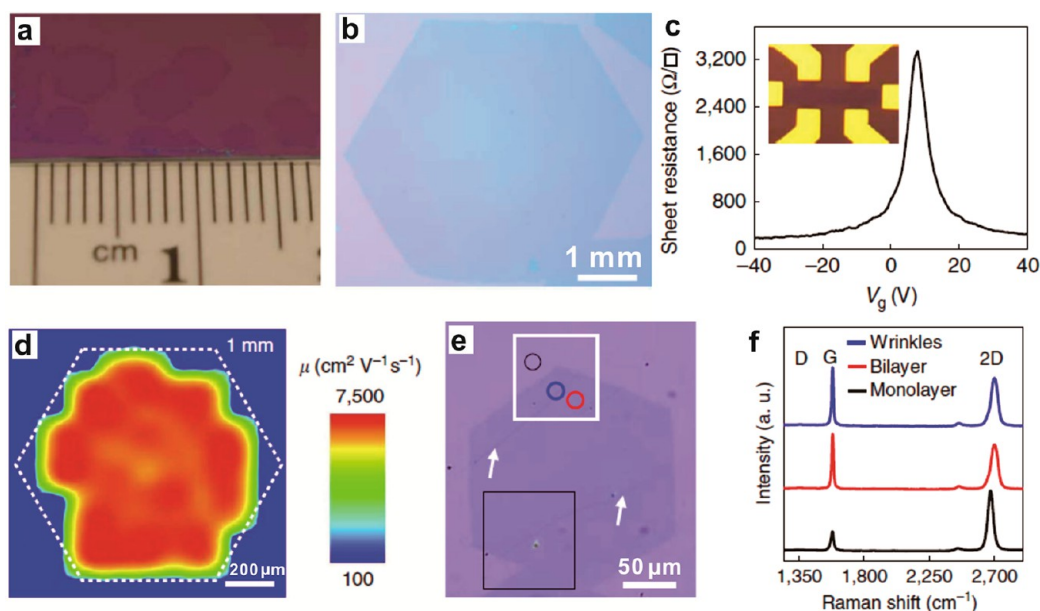


**Figure 5.** Millimeter-sized graphene grains made on oxygen-rich Cu. (a) Photograph and (b) optical microscopy image of millimeter-sized graphene grains. (c) Resistivity of graphene vs the back-gate voltage at room temperature. The inset is the optical microscopy image of a graphene Hall bar field effect transistor (FET) fabricated on a SiO<sub>2</sub>/Si substrate. (d) Two-dimensional color plot of the carrier (hole) mobility of a 55-FET-device array made on one single crystalline graphene grain. (e) Optical microscope image of a graphene grain with bilayer region transferred onto SiO<sub>2</sub>/Si wafer. (f) Raman spectra taken from the marked spots in panel (e). Adapted with permission from Macmillan Publishers Ltd. (*Nat. Commun.*),<sup>27</sup> copyright 2013.

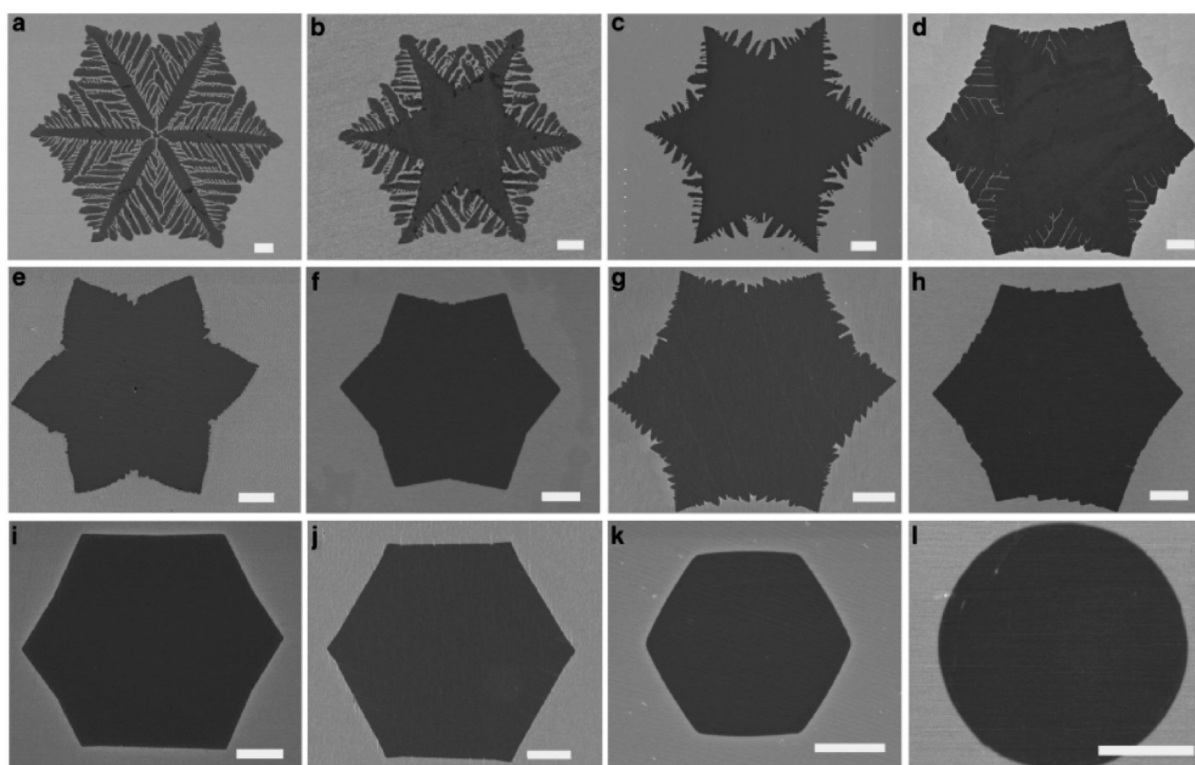


**Figure 6.** SEM images of a series of graphene grains grown on liquid Cu surfaces with different shapes that are engineered by varying the Ar/H<sub>2</sub> ratio. All scale bars are 5 μm. Reproduced with permission from Macmillan Publishers Ltd. (*NPG, Asia Mater.*),<sup>32</sup> copyright 2013.

also used AFM to explain why graphene nucleation could be suppressed on the resolidified Cu. Figure 4b and c indicates that the resolidified Cu (root-mean-square (RMS): ~8 nm) has a much smoother surface than that of the as-received Cu (RMS: ~166 nm). This further demonstrated that Cu surface

morphology is one of the most important factors influencing graphene nucleation densities.

#### 2.4. Millimeter-Sized Monolayer Graphene Single Crystals Made on Oxygen-Rich Cu Foils

These three methods focused mainly on the smoothing and improvement of the Cu surfaces to suppress graphene



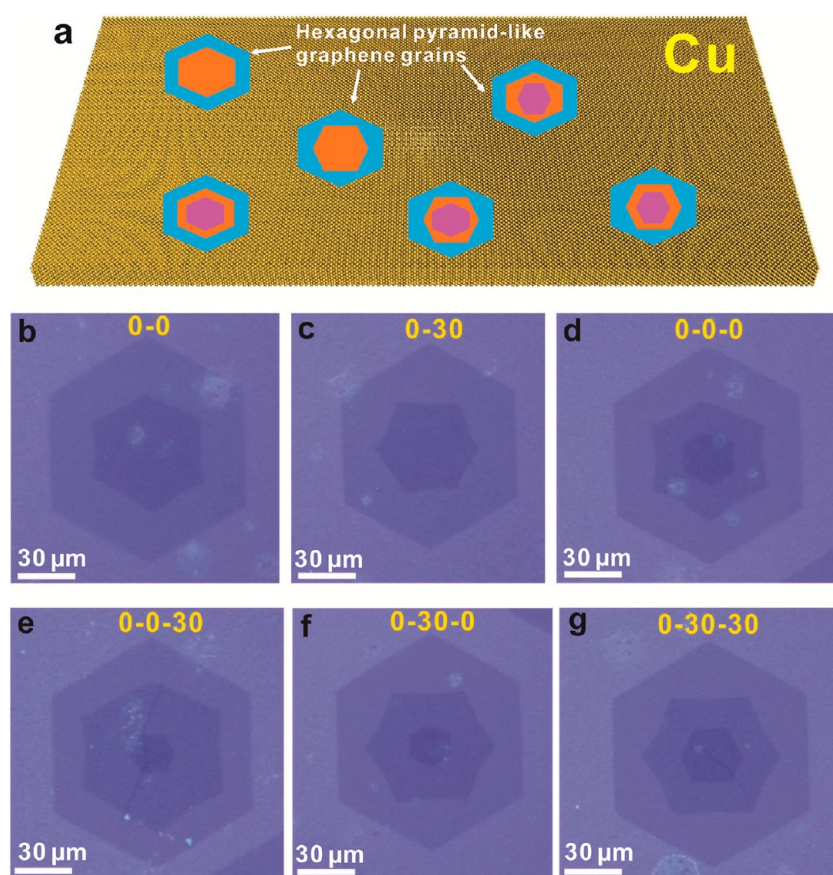


**Figure 7.** Hexagonal pyramid-like bi- and trilayer graphene single crystals made on Cu foils. (a) Scheme of bi- and trilayer graphene single crystals synthesized on Cu. (b–g) Representative optical images of pyramid-like bi- and trilayer graphene single crystals on SiO<sub>2</sub> (100 nm)/Si substrates. Adapted with permission,<sup>35</sup> copyright © 2013 WILEY-VCH Verlag GmbH & Co. KGaA, Weinheim.

nucleation. Most recently, Duan et al. reported a different pathway to make millimeter-sized single-crystal graphene grains.<sup>27</sup> The authors annealed Cu foils in a nonreducing gas (Ar) to maintain a catalytically inactive Cu<sub>2</sub>O layer. They found that the presence of the Cu<sub>2</sub>O layer suppressed the graphene nucleus density by more than 5 orders of magnitude, to reach an ultralow density of 4 nuclei cm<sup>-2</sup>. After 48 h of growth, ~5 mm sized hexagonal monolayer graphene grains with straight edges were synthesized (Figure 5a,b). Such graphene grains exhibit excellent electronic properties with a carrier mobility up to 16 000 cm<sup>2</sup> V<sup>-1</sup> s<sup>-1</sup> (Figure 5c).

Grain boundaries are known to be a primary factor responsible for the device-to-device variation in polycrystalline CVD graphene-based fabrication. The authors conducted mobility mapping on the as-made single-crystal graphene grains, showing an excellent device-to-device uniformity (Figure 5d). Moreover, the authors also demonstrated the synthesis of ~300 μm sized AB-stacked bilayer graphene single crystals using monolayer graphene grains as templates.

Interestingly, after the publication of Duan's research, the Luo<sup>28</sup> and Ruoff<sup>17</sup> laboratories also reported the suppression of graphene nucleation by oxygen-rich Cu. Through oxygen treatment of the Cu foil prior to graphene growth, Ruoff synthesized centimeter-scale single-crystal graphene grains.<sup>17</sup>

### 3. GRAPHENE SINGLE CRYSTALS WITH SPECIAL SPATIAL STRUCTURES MADE ON Cu

As an important 2D layered material, the properties of graphene can be controlled by its shape, size, thickness and edge structure. Thus, controlling growth parameters to make single-crystal graphene grains with special spatial structures is important not only for potential applications of graphene but also for understanding the growth mechanism of graphene and graphene-like 2D layered materials. In this section, we will review recent research on the synthesis of graphene grains with interesting spatial structures.

#### 3.1. Monolayer Graphene Single Crystals with Different Shapes

According to first-principle calculations, graphene grains should have compact hexagonal shapes at kinetic equilibrium because zigzag edges grow slowest on Cu substrates.<sup>15</sup> Interestingly, recent research demonstrates that graphene grains can exhibit a variety of other regular shapes in addition to hexagons, such as squares, snowflakes and flowers, by changing growth parameters to disturb the kinetic equilibrium.<sup>29–32</sup>

The shape of graphene grains can be influenced by various growth parameters, such as growth pressure,<sup>30</sup> ratio of H<sub>2</sub> to CH<sub>4</sub>,<sup>31</sup> and ratio of Ar to H<sub>2</sub>.<sup>32</sup> For example, Wu et al. demonstrated the precise tailoring of graphene grain shapes by varying ratios of Ar and H<sub>2</sub> (Figure 6) using CH<sub>4</sub> as the carbon source.<sup>32</sup> The authors found that, by using higher ratios of Ar to H<sub>2</sub>, graphene grains with a symmetric dendritic structure were formed (Figure 6a–d). As the ratio of Ar to H<sub>2</sub> was decreased,

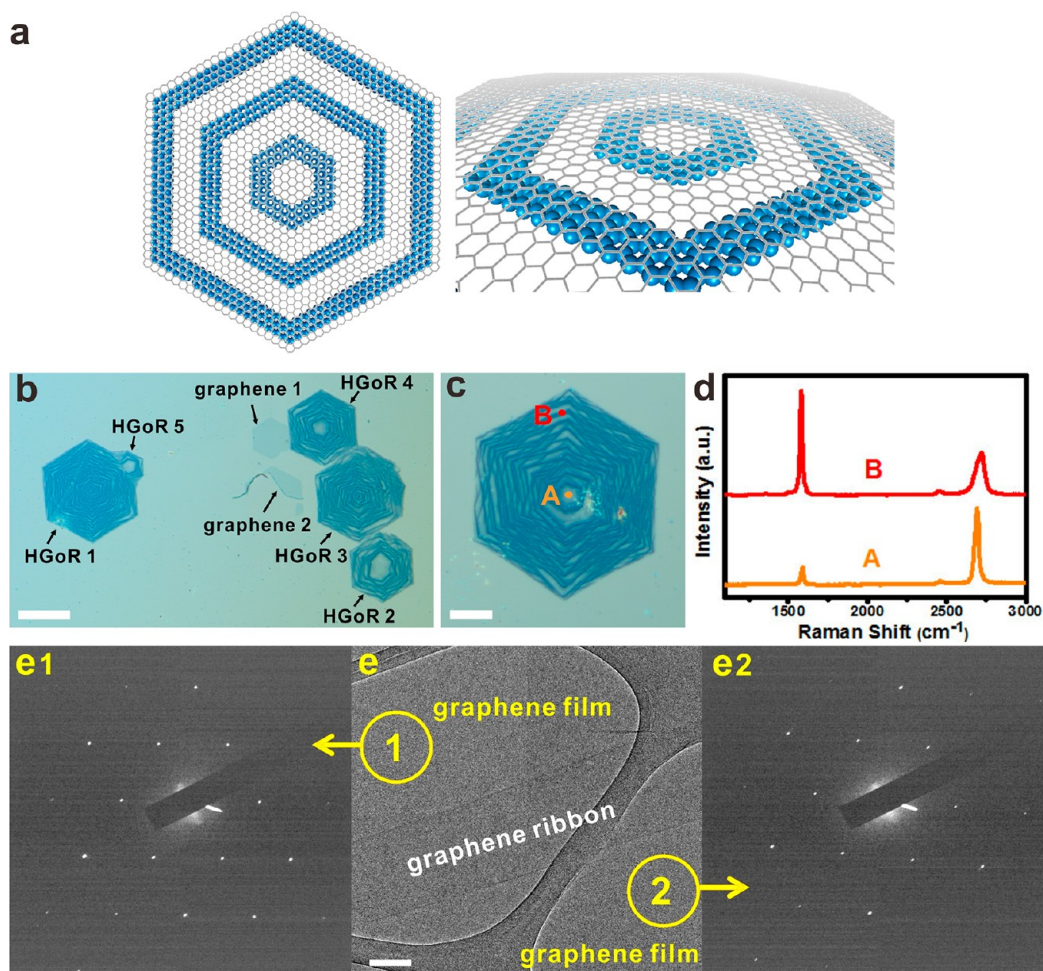


**Figure 8.** Hexagonal-onion-ring-like graphene single crystals (HGoR). (a) Top view and side view of the structural models of HGoR. (b,c) Optical images of HGoRs on SiO<sub>2</sub> (100 nm)/Si wafers. Scale bars are 50 and 20  $\mu\text{m}$ . (d) Raman spectra of point A and point B in (c). (e) Selected area electron diffraction patterns and the TEM image of one HGoR transferred onto a TEM grid. Scale bar is 100 nm. Reproduced with permission from ref 37. Copyright 2013 American Chemical Society.

more-compact structures appeared (Figure 6e–h), and, eventually, regular hexagonal graphene grains with straight edges were obtained (Figure 6i–k). The edges of the hexagonal graphene grains adopted a positive curvature upon increasing the CH<sub>4</sub> flow rate in a pure H<sub>2</sub> environment, eventually forming circular grains as shown in Figure 6l. Based on these interesting experimental observations, the exploration of the precise kinetic mechanism is an interesting topic and deserves more attention.

### 3.2. Hexagonal Pyramid-like Bi- and Trilayer Graphene Single Crystals

As a layered 2D material, graphene exhibits thickness- and stacking-dependent electronic properties.<sup>33,34</sup> Therefore, CVD synthesis of large bi- and trilayer graphene single crystals with controlled thickness and well-defined interlayer rotations would provide a material with both fundamental interests and practical applications.

We reported the fabrication of  $\sim 100\ \mu\text{m}$  pyramid-like bi- and trilayer graphene grains on Cu, which show hexagonal shapes and well-defined interlayer rotations on (Figure 7).<sup>35</sup> Optical images of the as-made graphene grains in Figure 7b–g indicate almost exclusively either 0° or 30° interlayer rotations. Depending on stacking orders, two types of bilayer graphene grains and four types of trilayer graphene grains were obtained (Figure 7b–g). Characterization by Raman spectroscopy, transmission electron

microscope (TEM), and Fourier transform infrared (FT-IR) spectroscopy with synchrotron radiation demonstrated that 0–0 bilayer graphene grains were Bernal stacked. The measured carrier (hole) mobility of the 0–0 bilayer graphene was  $\sim 5000\ \text{cm}^2\ \text{V}^{-1}\ \text{s}^{-1}$  at room temperature on SiO<sub>2</sub>/Si substrates, which was significantly higher than that of polycrystalline Bernal-stacked bilayer graphene.<sup>36</sup> Based on first-principle calculations, a graphene nucleation mechanism on Cu step edges was proposed, which could explain the origin of the interlayer rotations and also agrees well with the experimental observations.

### 3.3. Hexagonal-Onion-Ring-like Graphene Single Crystals

The growth of graphene on Cu is seed-induced 2D growth, limiting the fabrication of complex graphene spatial structures.<sup>14</sup> Most recently, we found that 3D growth of new graphene layers on the edges of the original graphene layer could be induced by controlling the H<sub>2</sub> partial pressure during the growth process.<sup>37</sup> Using this method, we successfully synthesized onion-ring-like 3D hexagonal graphene structures (hexagonal graphene onion rings, HGoRs), which are composed of concentric 1D few-layer graphene ribbon rings grown under 2D single-crystal monolayer graphene grains.

Figure 8a provides the structural models of HGoRs, and Figure 8b,c shows their typical optical images. The HGoR in Figure 8c was also characterized by Raman spectroscopy (Figure 8d).



From Figure 8d, it is apparent that the middle region (point A) of the HGoR was monolayer and the blue graphene ribbon rings (point B) of this part of the HGoR are multilayer, showing that the formation of HGoRs is based on the growth of few-layer graphene ribbons under monolayer graphene grains. TEM characterizations in Figure 8e indicate that a graphene nano-ribbon grew under a suspended single-crystal graphene film. From Figure 8e, one can see the graphene ribbon has smooth edges and its width is  $\sim 200$  nm. Two special features of HGoRs were also demonstrated in this work, including nanoribbon fabrication and potential use in lithium storage.

#### 4. MILLIMETER-SIZED MONOLAYER GRAPHENE GRAINS MADE ON OTHER METAL SUBSTRATES

Besides copper, other metal substrates, such as Ni,<sup>38</sup> Pt,<sup>39</sup> and Ru,<sup>40</sup> can also be used for the growth of millimeter-sized monolayer single-crystal graphene. For the Ni substrate, there is only 1.2% mismatch between crystal Ni(111) and graphene, making it a suitable substrate for the epitaxial growth of graphene. However, in most growth recipes, the carbon precipitation dominates the growth of graphene on Ni due to its high carbon solubility at growth temperatures, leading to the formation of few-layer polycrystalline graphene.<sup>9</sup>

To suppress the carbon precipitation, several modified growth procedures have been applied for the growth of monolayer single-crystal graphene on Ni.<sup>38,41,42</sup> For example, Iwasaki et al. realized the fabrication of monolayer graphene films with millimeter-sized grains on single-crystal Ni(111) films (Figure 9a).<sup>38</sup> In the growth process, low growth temperatures and

ultrahigh vacuum (UHV) were applied. Using this special growth protocol, the authors found that catalytic decomposition of carbon sources only occurs at the surface of Ni and the growth of graphene follows the orientation of the single-crystal Ni(111) film with high fidelity. A low energy electron diffraction (LEED) image taken after the growth shows that the as-made graphene had millimeter-sized grain sizes (the inset in Figure 9a). Figure 9b is a photograph of the as-made graphene transferred onto a SiO<sub>2</sub> wafer.

Several other groups also investigated using Ni to grow monolayer single-crystal graphene. For instance, under UHV condition,<sup>41</sup> the size and shape of graphene single crystals could be selected by controlling the postannealing time and temperature. In other work,<sup>42</sup> the authors cleverly put an Al<sub>2</sub>O<sub>3</sub> blocking layer in-between Ni and the solid carbon sources to prevent excess carbon from diffusing into Ni, and successfully synthesized  $\sim 100$   $\mu\text{m}$  sized monolayer graphene single crystals.

Other than Cu and Ni, noble metals have also been investigated for the growth of millimeter-sized single crystal graphene. On Pt foils, millimeter-sized hexagonal single-crystal graphene grains were successfully synthesized using the CVD method.<sup>39</sup> Due to the higher catalytic abilities of Pt for the dissociation of CH<sub>4</sub> than that of Cu, a high growth temperature (1040 °C) and a very low CH<sub>4</sub>/H<sub>2</sub> flow rate ratio (4/700) were used for the growth of large single-crystal graphene. Interestingly, the growth rate of graphene on Pt foils is  $\sim 4$   $\mu\text{m min}^{-1}$ , 4 times faster than that of graphene on Cu when similar growth conditions were applied. Figure 9c–e shows the SEM images of hexagonal graphene grains grown on Pt foils with increasing growth time, indicating that their sizes were roughly proportional to the growth time. Very recently, Cheng discovered that edges of single-crystal graphene domains grown on Pt can be tuned from zigzag to armchair via a CVD growth-etching-regrowth process.<sup>43</sup> This growth/etching behavior is well explained at the atomic level based on the concentrations of the kinks on various edges, providing a deep understanding of CVD graphene growth.

Single-crystal graphene could also be fabricated on a Ru(0001) substrate, with annealing at 1000 K under UHV condition ( $10^{-7}$  Pa).<sup>40</sup> The scanning tunneling microscope (STM) images in Figure 9f–h clearly show the hexagonal Moiré pattern, representing the interference between the lattices of the graphene and the underlying Ru(0001) surface. Another finding shown in Figure 9f–h is that the graphene can form continuously, regardless of the terraces and step edges of the Ru(0001) surface. This suggests the possibility of growing large-area graphene with no breakage of its structure or symmetry.

#### 5. SINGLE-CRYSTAL GRAPHENE GRAINS MADE ON INSULATING SUBSTRATES

While most CVD-derived graphene is grown on metal catalyst substrates, intensive research is also focused on transfer-free growth of graphene directly on insulating substrates, such as h-BN or SiO<sub>2</sub>.<sup>44</sup> Recently, Yang et al. reported the direct synthesis of single-crystal graphene grains on h-BN using a remote plasma-enhanced CVD process.<sup>45</sup> In the growth process, CH<sub>4</sub> was dissociated into reactive carbon radicals to nucleate and grow into graphene, as well as atomic hydrogen acting as etchant for ensuring sp<sup>2</sup> carbon growth (Figure 10a). Raman spectra determined the grown graphene to be monolayer graphene (MLG) or bilayer graphene (BLG) (Figure 10b). During the growth process, the underlying h-BN substrate played an important role in facilitating the epitaxial growth of graphene, as evidenced by the same orientations of the hexagonal graphene

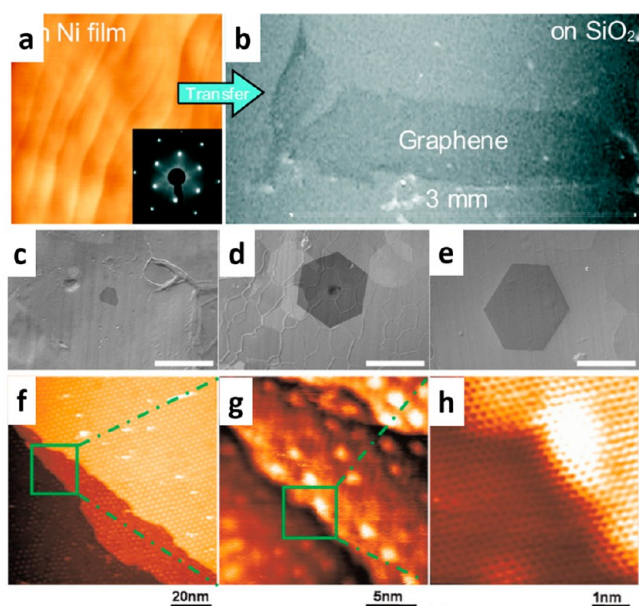


**Figure 9.** Single-crystal graphene grown on Ni, Pt and Ru. (a) One AFM image of single-crystal graphene grown on Ni and (b) one photograph image of a transferred graphene sample onto SiO<sub>2</sub>. The inset in panel (a) represents the LEED patterns of graphene synthesized on Ni film (Adapted with permission from ref 38. Copyright 2011 American Chemical Society). SEM images of graphene grains grown on Pt foils with different growth times of (c) 60, (d) 120, and (e) 180 min (Adapted with permission from Macmillan Publishers Ltd. (*Nat. Commun.*),<sup>39</sup> copyright 2012). (f–h) STM images of the graphene overlayer above Ru terrace edges (Adapted with permission,<sup>40</sup> copyright © 2009 WILEY-VCH Verlag GmbH & Co. KGaA, Weinheim). Scale bars in (c)–(e) are 400  $\mu\text{m}$ .

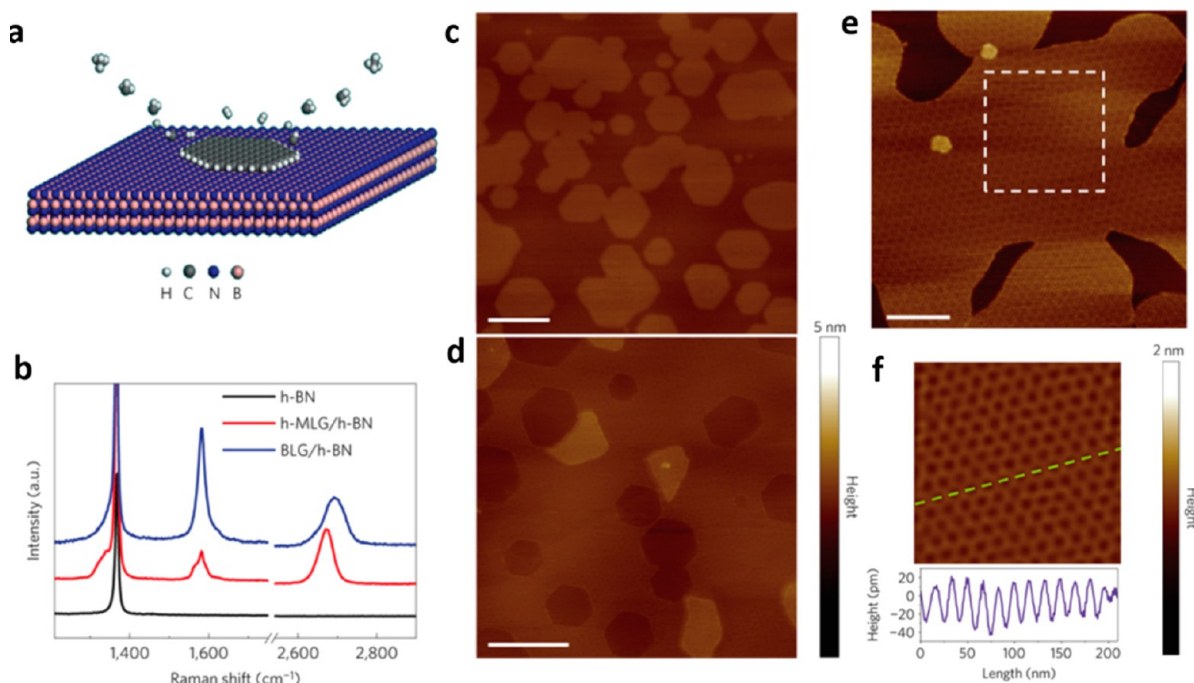


**Figure 10.** Epitaxial growth of single-crystal graphene on h-BN. (a) Schematic illustration of the growth mechanism. (b) Raman spectra for MLG/h-BN (red), BLG/h-BN (blue), and bare h-BN surface (black). (c, d) Enlarged AFM images of as-grown graphene showing (c) aligned hexagonal grains or (d) pits after plasma etching. (e) Moiré pattern of a coalesced grain. (f) High-pass-filtered inverse fast Fourier transform of the pattern in the dashed square in (e); the lower part is the height profile along the dashed line. Scale bars in (c, d) are 200 nm, and in (e, f) are 100 nm. Adapted with permission,<sup>45</sup> from Macmillan Publishers Ltd. (*Nat. Mater.*), copyright 2013.

grains shown in the AFM image (Figure 10c). Figure 10c also demonstrates that the grain sizes of the as-made graphene on h-BN were  $<1\ \mu\text{m}$ . Additionally, hexagonal pits with the same orientations were also observed after anisotropic etching of a continuous as-grown graphene film (Figure 10d). With this fixed stacking orientation between as-grown graphene and the underlying h-BN substrate, trigonal Moiré patterns could be seen using AFM analysis (Figure 10e,f). h-BN is an ideal substrate for graphene device fabrication.<sup>46</sup> Thus, this method of making graphene/BN heterostructures should have great potential in graphene electronic applications.

## 6. SUMMARY AND OUTLOOK

The CVD synthesis of large-size and grain-free graphene with controlled thickness and designed spatial structures is essential for both fundamental research and practical applications. In this Account, recent research in synthesizing millimeter-sized monolayer graphene grains on different substrates was reviewed in detail. The efforts in making graphene grains with controlled thicknesses and engineered spatial structures was also described. Finally, the recent breakthrough of directly growing graphene single crystals on h-BN was discussed.

Although great advancements have been achieved in CVD synthesis of graphene single crystals, potential challenges still exist. For instance, the synthesis of centimeter-sized up to wafer-scale graphene single crystals is required to minimize device-to-device variations and enable practical applications of graphene in electronics and optics. Their directional lithographic cutting might yield preferred edge orientations in confined structures. The production of larger and monodisperse sizes of graphene single crystals are important challenges that remain to be solved. In addition, a deep understanding of the graphene growth mechanism and growth dynamics is needed in order to make

graphene grains with precisely controlled thicknesses and spatial structures. Furthermore, another critical step is to directly grow high-quality and large single-crystal graphene on insulating substrates. Despite recent progress addressing this problem using a remote plasma-enhanced CVD process,<sup>45</sup> the as-made graphene single crystals have small sizes ( $<1\ \mu\text{m}$ ) and are limited to h-BN substrates. It would be of great interest if the direct growth of large-size and high-quality graphene single crystals with engineered spatial structures on different insulating substrates, such as h-BN, SiO<sub>2</sub> and ceramic, and semiconductors such as Si and GaAs, could be achieved. At the pace of worldwide research in this area, these desired advances are likely to come soon.

## AUTHOR INFORMATION

### Notes

The authors declare no competing financial interest.

### Biographies

**Dr. Zheng Yan** received his B.S. in chemical engineering from Xi'an Jiao Tong University, his M.S. in chemistry from Tsinghua University, and his Ph.D. in chemistry in 2013 from Rice University, working on chemical production of graphene and graphene-like 2D layered materials and their applications in electronics, optics, and alternative energy devices. Presently, he is a postdoctoral scholar at the University of Illinois at Urbana-Champaign.

**Zhiwei Peng** received his B.S. in chemistry from Peking University in China. He is currently a Ph.D. candidate in the chemistry department at Rice University. His current research interests include chemical production of carbon nanomaterials for energy, environmental, and optoelectronics applications.



**Dr. James M. Tour**, a synthetic organic chemist, is presently the T. T. and W. F. Chao Professor of Chemistry, Professor of Computer Science, and Professor of Mechanical Engineering and Materials Science. Tour's scientific research areas include a diversity of nanomaterials and nanomedicine topics. He was ranked one of the Top 10 chemists in the world over the past decade by a Thomson Reuters citations per publication index survey and he was named Chemist of the Year for 2013 by *R&D Magazine*. Tour has over 500 research publications and over 60 patents. <http://www.jmtour.com>.

## ■ ACKNOWLEDGMENTS

The work at Rice University was supported by the ONR MURI program (#00006766, N00014-09-1-1066), AFOSR MURI (FA9550-12-1-0035), and the AFOSR (FA9550-09-1-0581). The authors thank E. L. G. Samuel for drawing the TOC.

## ■ REFERENCES

- (1) Novoselov, K. S.; Geim, A. K.; Morozov, S. V.; Jiang, D.; Zhang, Y.; Dubonos, S. V.; Grigorieva, I. V.; Firsov, A. A. Electric Field Effect in Atomically Thin Carbon Films. *Science* **2004**, *306*, 666–669.
- (2) Novoselov, K. S.; Geim, A. K.; Morozov, S. V.; Jiang, D.; Katsnelson, M. I.; Grigorieva, I. V.; Dubonos, S. V.; Firsov, A. A. Two-Dimensional Gas of Massless Dirac Fermions in Graphene. *Nature* **2005**, *438*, 197–200.
- (3) Zhang, Y. B.; Tan, Y. W.; Stormer, H. L.; Kim, P. Experimental Observation of the Quantum Hall Effect and Berry's Phase in Graphene. *Nature* **2005**, *438*, 201–204.
- (4) Geim, A. K.; Novoselov, K. S. The Rise of Graphene. *Nat. Mater.* **2007**, *6*, 183–191.
- (5) Dreyer, D. R.; Park, S.; Bielawski, C. W.; Ruoff, R. S. The Chemistry of Graphene Oxide. *Chem. Soc. Rev.* **2010**, *39*, 228–240.
- (6) Waldmann, D.; Jobst, J.; Speck, F.; Seyller, T.; Krieger, M.; Weber, H. B. Bottom-Gated Epitaxial Graphene. *Nat. Mater.* **2011**, *10*, 357–360.
- (7) Reina, A.; Jia, X.; Ho, J.; Nezich, D.; Son, H.; Bulovic, V.; Dresselhaus, M. S.; Kong, J. Large-Area, Few-Layer Graphene Films on Arbitrary Substrates by Chemical Vapor Deposition. *Nano Lett.* **2009**, *9*, 30–35.
- (8) Li, X.; Cai, W.; An, J.; Kim, S.; Nah, J.; Yang, D.; Piner, R.; Velamakanni, A.; Jung, I.; Tutuc, E.; Banerjee, S. K.; Colombo, L.; Ruoff, R. S. Large-Area Synthesis of High-Quality and Uniform Graphene Films on Copper Foils. *Science* **2009**, *324*, 1312–1314.
- (9) Kim, K. S.; Zhao, Y.; Jang, H.; Lee, S. Y.; Kim, J. M.; Kim, K. S.; Ahn, J.-H.; Kim, P.; Choi, J.-Y.; Hong, B. H. Large-Scale Pattern Growth of Graphene Films for Stretchable Transparent Electrodes. *Nature* **2009**, *457*, 706–710.
- (10) Bae, S.; Kim, H.; Lee, Y.; Xu, X.; Park, J.-S.; Zheng, Y.; Balakrishnan, J.; Lei, T.; Kim, H. R.; Song, Y.; Il, Kim, Y.-K.; Kim, K. S.; Ozyilmaz, B.; Ahn, J.-H.; Hong, B. H.; Iijima, S. Roll-to-Roll Production of 30-Inch Graphene Films for Transparent Electrodes. *Nat. Nanotechnol.* **2010**, *5*, 574–578.
- (11) Huang, P. Y.; Ruiz-Vargas, C. S.; van der Zande, A. M.; Whitney, W. S.; Levendorf, M. P.; Kevek, J. P.; Garg, S.; Alden, J. S.; Hustedt, C. J.; Zhu, Y.; Park, J.; McEuen, P. L.; Muller, D. A. Grains and Grain Boundaries in Single-Layer Graphene Atomic Patchwork Quilts. *Nature* **2011**, *469*, 389–392.
- (12) Tsen, A. W.; Brown, L.; Levendorf, M. P.; Ghahari, F.; Huang, P. Y.; Havener, R. W.; Ruiz-Vargas, C. S.; Muller, D. A.; Kim, P.; Park, J. Tailoring Electrical Transport Across Grain Boundaries in Polycrystalline Graphene. *Science* **2012**, *336*, 1143–1146.
- (13) Ruiz-Vargas, C. S.; Zhuang, H. L.; Huang, P. Y.; van der Zande, A. M.; Garg, S.; McEuen, P. L.; Muller, D. A.; Hennig, R. G.; Park, J. Softened Elastic Response and Unzipping in Chemical Vapor Deposition Graphene Membranes. *Nano Lett.* **2011**, *11*, 2259–2263.
- (14) Yu, Q.; Jauregui, L. A.; Wu, W.; Colby, R.; Tian, J.; Su, Z.; Cao, H.; Liu, Z.; Pandey, D.; Wei, D.; Chung, T. F.; Peng, P.; Guisinger, N. P.; Stach, E. A.; Bao, J.; Pei, S.-S.; Chen, Y. P. Control and Characterization of Individual Grains and Grain Boundaries in Graphene Grown by Chemical Vapor Deposition. *Nat. Mater.* **2011**, *10*, 443–449.
- (15) Artyukhov, V. I.; Liu, Y.; Yakobson, B. I. Equilibrium at the Edge and Atomistic Mechanisms of Graphene Growth. *Proc. Natl. Acad. Sci. U.S.A.* **2012**, *109*, 15136–15140.
- (16) Sun, Z.; Yan, Z.; Jun, Y.; Beitler, E.; Zhu, Y.; Tour, J. M. Growth of Graphene from Solid Carbon Sources. *Nature* **2010**, *468*, 549–552.
- (17) Hao, Y.; Bharathi, M. S.; Wang, L.; Liu, Y.; Chen, H.; Nie, S.; Wang, X.; Chou, H.; Tan, C.; Fallahazad, B.; Ramanarayan, H.; Magnuson, C. W.; Tutuc, E.; Yakobson, B. I.; McCarty, K. F.; Zhang, Y. W.; Kim, P.; Hone, J.; Colombo, L.; Ruoff, R. S. The Role of Surface Oxygen in the Growth of Large Single-Crystal Graphene on Copper. *Science* **2013**, *342*, 720–723.
- (18) Vlassioudis, I.; Regmi, M.; Fulvio, P.; Dai, S.; Datskos, P.; Eres, G.; Smirnov, S. Role of Hydrogen in Chemical Vapor Deposition Growth of Large Single-Crystal Graphene. *ACS Nano* **2011**, *5*, 6069–6076.
- (19) Gao, L.; Guest, J. R.; Guisinger, N. P. Epitaxial Graphene on Cu(111). *Nano Lett.* **2010**, *10*, 3512–3516.
- (20) Yan, Z.; Lin, J.; Peng, Z.; Sun, Z.; Zhu, Y.; Li, L.; Xiang, C.; Samuel, E. L.; Kittrell, C.; Tour, J. M. Toward the Synthesis of Wafer-Scale Single-Crystal Graphene on Copper Foils. *ACS Nano* **2012**, *6*, 9110–9117.
- (21) Wu, T.; Ding, G.; Shen, H. L.; Wang, H. M.; Sun, L.; Jiang, D.; Xie, X. M.; Jiang, M. H. Triggering the Continuous Growth of Graphene Toward Millimeter-Sized Grains. *Adv. Funct. Mater.* **2013**, *23*, 198–203.
- (22) Li, X.; Magnuson, C. W.; Venugopal, A.; Tromp, R. M.; Hannon, J. B.; Vogel, E. M.; Colombo, L.; Ruoff, R. S. Large-Area Graphene Single Crystals Grown by Low-Pressure Chemical Vapor Deposition of Methane on Copper. *J. Am. Chem. Soc.* **2011**, *133*, 2816–2819.
- (23) Chen, S.; Ji, H.; Chou, H.; Li, Q.; Li, H.; Suk, J. W.; Piner, R.; Liao, L.; Cai, W.; Ruoff, R. S. Millimeter-Size Single-Crystal Graphene by Suppressing Evaporative Loss of Cu During Low Pressure Chemical Vapor Deposition. *Adv. Mater.* **2013**, *25*, 2062–2065.
- (24) Geng, D.; Wu, B.; Guo, Y.; Huang, L.; Xue, Y.; Chen, J.; Yu, G.; Jiang, L.; Hu, W.; Liu, Y. Uniform Hexagonal Graphene Flakes and Films Grown on Liquid Copper Surface. *Proc. Natl. Acad. Sci. U.S.A.* **2012**, *109*, 7992–7996.
- (25) Wu, Y. A.; Fan, Y.; Speller, S.; Creeth, G. L.; Sadowski, J. T.; He, K.; Robertson, A. W. Large Single Crystals of Graphene on Melted Copper Using Chemical Vapor Deposition. *ACS Nano* **2012**, *6*, 5010–5017.
- (26) Mohsin, A.; Liu, L.; Liu, P.; Deng, W.; Ivanov, I. N.; Li, G.; Dyck, O. E.; Duscher, G.; Dunlap, J. R.; Xiao, K.; Gu, G. Synthesis of Millimeter-Size Hexagon-Shaped Graphene Single Crystals on Resolidified Copper. *ACS Nano* **2013**, *7*, 8924–8931.
- (27) Zhou, H.; Yu, W. J.; Liu, L.; Cheng, R.; Chen, Y.; Huang, X.; Liu, Y.; Wang, Y.; Huang, Y.; Duan, X. Chemical Vapor Deposition Growth of Large Single Crystals of Monolayer and Bilayer Graphene. *Nat. Commun.* **2013**, DOI: 10.1038/ncomms3096.
- (28) Gan, L.; Luo, Z. Turning off Hydrogen to Realize Seeded Growth Subcentimeter Single-Crystal Graphene Grains on Copper. *ACS Nano* **2013**, *7*, 9480–9488.
- (29) Wang, H.; Wang, G.; Bao, P.; Yang, S.; Xie, X.; Zhang, W. Controllable Synthesis of Submillimeter Single-Crystal Monolayer Graphene Domains on Copper Foils by Suppressing Nucleation. *J. Am. Chem. Soc.* **2012**, *134*, 3627–3630.
- (30) Zhang, Y.; Zhang, L.; Kim, P.; Ge, M.; Li, Z.; Zhou, C. Vapor Trapping Growth of Single-Crystalline Graphene Flowers: Synthesis, Morphology, and Electronic Properties. *Nano Lett.* **2012**, *12*, 2810–2816.
- (31) Jacobberger, R. M.; Arnold, M. S. Graphene Growth Dynamics on Epitaxial Copper Thin Films. *Chem. Mater.* **2013**, *25*, 871–877.
- (32) Wu, B.; Geng, D.; Xu, Z.; Guo, Y.; Huang, L.; Xue, Y.; Chen, J.; Yu, G.; Liu, Y. Self-Organized Graphene Crystal Patterns. *NPG Asia Mater.* **2013**, DOI: 10.1038/am.2012.68.
- (33) Zhang, Y.; Tang, T. T.; Girit, C.; Hao, Z.; Martin, M. C.; Zettl, A.; Crommie, M. F.; Shen, Y. R.; Wang, F. Direct Observation of a Widely Tunable Bandgap in Bilayer Graphene. *Nature* **2009**, *459*, 820–823.



- (34) Lui, C.; Li, Z.; Mak, K. F.; Cappelluti, E.; Heinz, T. F. Observation of an Electrical Tunable Band Gap in Trilayer Graphene. *Nat. Phys.* **2011**, *7*, 944–947.
- (35) Yan, Z.; Liu, Y.; Ju, L.; Peng, Z.; Lin, J.; Wang, G.; Zhou, H.; Xiang, C.; Samuel, E. L. G.; Kittrell, C.; Artyukhov, V. I.; Wang, F.; Yakobson, B. I.; Tour, J. M. Large Hexagonal Bi- and Trilayer Graphene Single Crystals with Varied Interlayer Rotations. *Angew. Chem., Int. Ed.* **2014**, *53*, 1565–1569.
- (36) Lee, S.; Lee, K.; Zhong, Z. Wafer Scale Homogeneous Bilayer Graphene Films by Chemical Vapor Deposition. *Nano Lett.* **2010**, *10*, 4702–4707.
- (37) Yan, Z.; Liu, Y.; Lin, J.; Peng, Z.; Wang, G.; Pembroke, E.; Zhou, H.; Xiang, C.; Raji, A. O.; Samuel, E. L. G.; Yu, T.; Yakobson, B. I.; Tour, J. M. Hexagonal Graphene Onion Rings. *J. Am. Chem. Soc.* **2013**, *135*, 10755–10762.
- (38) Iwasaki, T.; Park, H. J.; Konuma, M.; Lee, D. S.; Smet, J. H.; Starke, U. Long-Range Ordered Single-Crystal Graphene on High-Quality Heteroepitaxial Ni Thin Films Grown on MgO(111). *Nano Lett.* **2011**, *11*, 79–84.
- (39) Gao, L.; Ren, W.; Xu, H.; Jin, L.; Wang, Z.; Ma, T.; Ma, L.; Zhang, Z.; Fu, Q.; Peng, L.; Bao, X.; Cheng, H. Repeated Growth and Bubbling Transfer of Graphene with Millimeter-size Single-crystal Grains using Platinum. *Nat. Commun.* **2012**, *3*, 699.
- (40) Pan, Y.; Zhang, H.; Shi, D.; Sun, J.; Du, S.; Liu, F.; Gao, H. Highly Ordered, Millimeter-Scale, Continuous, Single-Crystalline Graphene Monolayer Formed on Ru(0001). *Adv. Mater.* **2008**, *20*, 1–4.
- (41) Olle, M.; Ceballos, G.; Serrate, D.; Gambardella, P. Yield and Shape Selection of Graphene Nanoislands Grown on Ni(111). *Nano Lett.* **2012**, *12*, 4431–4436.
- (42) Weatherup, R. S.; Baehtz, C.; Dlubak, B.; Bayer, B. C.; Kidambi, P. R.; Blume, R.; Schloegl, R.; Hofmann, S. Introducing Carbon Diffusion Barriers for Uniform, High-Quality Graphene growth from Solid Sources. *Nano Lett.* **2013**, *13*, 4624–4631.
- (43) Ma, T.; Ren, W.; Zhang, X.; Liu, Z.; Gao, Y.; Yin, L.; Ma, X.; Ding, F.; Cheng, H. Edge-Controlled Growth and Kinetics of Single-Crystal Graphene Domains by Chemical Vapor Deposition. *Proc. Natl. Acad. Sci. U.S.A.* **2013**, *110*, 20386–20391.
- (44) Yan, Z.; Peng, Z.; Sun, Z.; Yao, J.; Zhu, Y.; Liu, Z.; Ajayan, P. M.; Tour, J. M. Growth of Bilayer Graphene on Insulating Substrates. *ACS Nano* **2011**, *5*, 8187–8192.
- (45) Yang, W.; Chen, G.; Shi, Z.; Liu, C.; Zhang, L.; Xie, G.; Cheng, M.; Wang, D.; Yang, R.; Shi, D.; Watanabe, K.; Taniguchi, T.; Yao, Y.; Zhang, Y.; Zhang, G. Epitaxial Growth of Single-Domain graphene on Hexagonal Boron Nitride. *Nat. Mater.* **2013**, *12*, 792–797.
- (46) Dean, C. R.; Young, A. F.; Meric, I.; Lee, C.; Wang, L.; Sorgenfrei, S.; Watanabe, K.; Taniguchi, T.; Kim, P.; Shepard, K. L.; Hone, J. Boron Nitride Substrates for High-Quality Graphene Electronics. *Nat. Nanotechnol.* **2010**, *5*, 722–726.